Inorganic Chemistry

Article

pubs.acs.org/IC

Silver Pyroarsonates Obtained from Ag(I)-Mediated in Situ Condensation of Aryl Arsonate Ligands under Solvothermal Conditions

Xiang-Ying Qian,[†,‡] Jun-Ling Song,[†] and Jiang-Gao Mao*[,†]

[†]State Key Laboratory of Structural Chemistry, Fujian Institute of Research on the Structure of Matter, Chinese Academy of Sciences, Fuzhou 350002, People's Republic of China

[‡]Graduate School of the Chinese Academy of Sciences, Beijing, 100039, People's Republic of China

Supporting Information

ABSTRACT: Four new layered silver(I) organoarsonates, namely, $[Ag_3(L^3)(CN)]$ (**1**) (H_2L^3 = $(PhAsO_2H)_2O$), $[Ag_3(L^4)(CN)]$ (**2**) (H_2L^4 = $(2\text{-}NO_2\text{-}C_6H_4\text{-}AsO_2H)_2O$), $[Ag_3(HL^5)(H_2L^5)]$ (**3**) (H_3L^5 = 3-NO_2-4-OH-C_6H_3-AsO_3H_2) and $[Ag_2(HL^5)]$ (**4**), were synthesized under solvothermal conditions. During the preparations of **1** and **2**, condensation of organoarsonate ligands (H_2L^1 = Ph-AsO_3H_2; H_2L^2 = 2-NO_2-C_6H_4-AsO_3H_2) and the decomposition of acetonitrile molecules to cyanide anions occurred. Single crystals of H_2L^4 ligand and compounds **1**−**4** were isolated, and their crystal structures have been determined by single crystal X-ray diffraction studies. In **1**, the one-dimensional (1D) chains based on Ag(I) ions and $\{L^3\}^{2-}$ anions are further interconnected by CN^- into two-dimensional (2D) layers. In **2**, adjacent Ag(I) ions within the silver(I) organoarsonate layer are further bridged by μ_4-CN^- anions with very short Ag···Ag contacts. In **3**, the hexanuclear $\{Ag_6O_{12}\}$ clusters are interconnected by bridging organoarsonate ligands into a silver(I) arsonate hybrid layer. In **4**, the right-handed $\{Ag_4O_4\}$ chains are further interconnected by organoarsonate ligands as well as additional Ag−O−Ag bridges into a novel silver(I) arsonate layer. Compounds **1** and **2** display red and orange-red emissions, respectively, which may be assigned to be an admixture of ligand-to-metal charge transfer (LMCT) and metal-centered (4d-5s/5p) transitions perturbed by Ag(I)···Ag(I) interactions. Upon cooling from room temperature to 10 K, compound **1** exhibits interesting temperature-dependent emissions.

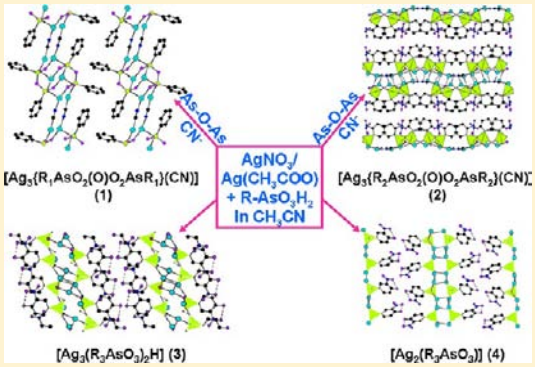

INTRODUCTION

Metal phosphonates have attracted tremendous research interest in the past 20 years because of their potential applications in optics, ion-exchange, catalysis, and sensors, and so forth.[1,2] Metal arsonates are expected to display a similar structural chemistry to those of metal phosphonates, but the larger ionic radius of As(V) than that of P(V) could possibly lead to some different architectures with different physical properties. So far, studies on metal arsonates are still limited. A variety of polyoxometalate clusters of vanadium, molybdenum, and tungsten capped by arsonate ligands have been reported.[3−6] A heteropoly-13-palladium(II) cluster of phenylarsonate ligand has also been isolated.[7] By using the solvothermal approach, Ma's group have prepared a series of organo oxo tin clusters of organoarsonates and several organotin arsonates with infinite ladders or chains.[8] By introducing an *O*-donor second metal linker of 5-sulfoisophthalic acid monosodium salt or 1,3,5-benzenetricarboxylic acid, three novel mixed-ligand lead(II) carboxylate-arsonates had been isolated by our group.[9] Using an *N*-donor chelating auxiliary ligand such as phen, 2,2′-bipy, or terpy led to the isolation of a series of divalent transition metal arsonates with various types of structures ranging from isolated clusters, one-dimensional (1D) chains to two-dimensional (2D) layers.[10] More interestly, when a flexible group of $-NHCH_2COOH$ was attached to the arsonic ligand, a layered chiral zinc(II) arsonate was obtained.[11] Very recently, a series of lanthanide arsonates had also been structurally characterized by our group.[12]

Silver-containing materials have received considerable interest because of their remarkable luminescent and catalytic properties for numerous chemical processes.[13,14] So far, no silver arsonate has been structurally characterized. Therefore, we started a research program to systematically study the structures and physical properties of silver organoarsonates. The solvothermal reaction of $AgNO_3$ with phenylarsonic acid (H_2L^1 = $PhAsO_3H_2$) or 2-nitrophenylarsonic acid (H_2L^2 = 2-NO_2-C_6H_4-AsO_3H_2) in acetonitrile resulted in $[Ag_3(L^3)(CN)]$ (**1**) (H_2L^3 = $(PhAsO_2H)_2O$) and $[Ag_3(L^4)(CN)]$ (**2**) (H_2L^4 = $(2\text{-}NO_2\text{-}C_6H_4\text{-}AsO_2H)_2O$), respectively, in which unexpected dimerization of the arsonate ligands (Scheme 1) and the decomposition of acetonitrile molecules into cyanide anions

Received: September 4, 2012
Published: February 6, 2013

dx.doi.org/10.1021/ic301935g | *Inorg. Chem.* 2013, 52, 1843−1853

Scheme 1. Free Ligands of H_2L^1, H_2L^2, H_3L^5 and the Corresponding Condensation Ligands of H_2L^3 and H_2L^4

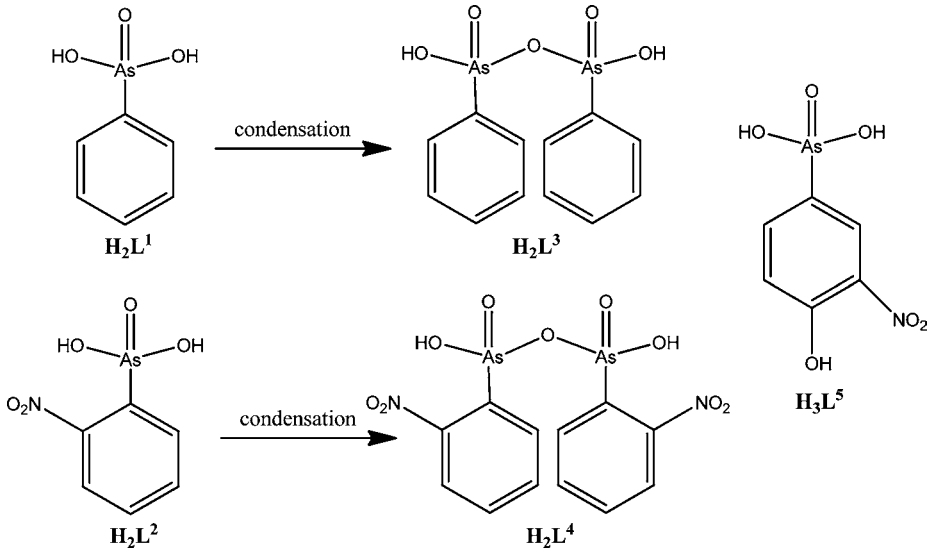

Table 1. Summary of Crystal Data and Structure Refinements for H_2L^4 and Compounds 1−4

compound	H_2L^4	1	2	3	4
formula	$C_{12}H_{10}As_2N_2O_9$	$C_{13}H_{10}Ag_3As_2NO_5$	$C_{13}H_8Ag_3As_2N_3O_9$	$C_{12}H_9Ag_3As_2N_2O_{12}$	$C_{12}H_8Ag_4As_2N_2O_{12}$
fw	476.06	733.67	823.67	846.66	953.52
space group	*Pbcn*	$P\bar{1}$	$P2_1/c$	$P\bar{1}$	$P2_1$
a [Å]	8.436(5)	5.939(3)	15.988(5)	6.680(3)	10.409(11)
b [Å]	7.843(5)	11.086(5)	15.673(4)	8.387(3)	5.664(6)
c [Å]	23.140(14)	12.822(6)	7.460(2)	17.250(7)	16.460(19)
α [deg]	90	84.902(9)	90	79.226(11)	90
β [deg]	90	87.198(11)	93.839(5)	87.677(10)	94.059(19)
γ [deg]	90	84.968(9)	90	79.746(9)	90
V [Å^3]	1531.1(15)	836.9(6)	1865.2(9)	934.1(6)	968.1(18)
Z	4	2	4	2	2
D_{calcd} [g·cm^{-3}]	2.065	2.911	2.933	3.010	3.271
μ(Mo Kα) (mm^{-1})	4.419	7.422	6.697	6.700	7.448
GOF on F^2	1.045	0.955	1.030	1.104	1.039
R1, wR2 [$I > 2\sigma(I)$]^a	0.0349, 0.0835	0.0320, 0.0564	0.0454, 0.0940	0.0513, 0.0824	0.0668, 0.1256
R1, wR2 (all data)^a	0.0410, 0.0870	0.0425, 0.0603	0.0626, 0.1035	0.0693, 0.0915	0.0988, 0.1453

^{a}R1 = $\sum||F_o| - |F_c||/\sum|F_o|$, wR2 = $\{\sum w[(F_o)^2 - (F_c)^2]^2/\sum w[(F_o)^2]^2\}^{1/2}$.

occurred. By selecting 4-hydroxy-3-nitrophenylarsonic acid as the arsonic ligand and $Ag(CH_3COO)$ as the Ag^+ source, $[Ag_3(HL^5)(H_2L^5)]$ (**3**) (H_3L^5 = 3-NO_2-4-OH-C_6H_3-AsO_3H_2) and $[Ag_2(HL^5)]$ (**4**) were isolated. They form four different types of layered structures. Herein, we report their syntheses, crystal structures, and luminescent properties.

EXPERIMENTAL SECTION

Materials and Methods. All chemicals except that of acetonitrile were obtained from commercial sources and used without further purification. Acetonitrile was dried with a 4 Å molecular sieve prior to use. Elemental analyses were performed on a German Elementary Vario EL III instrument. The FT−IR spectra were recorded on a Nicolet Magna 750 FT−IR spectrometer using KBr pellets in the range of 4000−400 cm^{-1}. Thermogravimetric analyses were carried out on a NETZSCH STA 449F unit at a heating rate of 10 °C/min under an oxygen atmosphere. X-ray powder diffraction (XRD) patterns (Cu−Kα) were collected on a Rigaku MiniFlex II diffractometer. Photoluminescence studies for compounds **1** and **2** were performed on an Edinburgh FLS920 fluorescent spectrometer.

Synthesis of $[Ag_3(L^3)(CN)]$ (1). A mixture of $AgNO_3$ (0.3 mmol) and phenylarsonic acid (0.2 mmol) in 2 mL of acetonitrile was sealed to a Parr Teflon-lined autoclave (23 mL) and heated at 140 °C for 6 days. Crystals of **1** were obtained as the major phase with a small amount of unidentified yellow impurity. The impurity was removed through ultrasound vibration and sieving. The crystals were recovered in about 54% yield (based on phenylarsonic acid), and the purity of the sample was confirmed by powder XRD (Supporting Information, Figure S1). Elem. anal. calcd (%) for $C_{13}H_{10}O_5NAs_2Ag_3$ (M_r = 733.67): C, 21.28; H, 1.37; N, 1.91. Found: C, 21.10; H, 1.55; N, 2.06. IR data for **1** (KBr, cm^{-1}): 3054(m), 2343(m), 2139(w), 1600(m), 1484(w), 1438(s), 1385(w), 1221(m), 1095(m), 906(s), 738(s), 693(m), 474(m).

Synthesis of $[Ag_3(L^4)(CN)]$ (2) and H_2L^4. A mixture of $AgNO_3$ (0.2 mmol) and 2-nitrophenylarsonic acid (0.1 mmol) in 2 mL of acetonitrile was sealed to a Parr Teflon-lined autoclave (23 mL) and heated at 120 °C for 2 days, then cooled to room temperature (RT) slowly. A mixture of two types of single crystals, $[Ag_3(L^4)(CN)]$ and H_2L^4, were obtained. When the reaction time was prolonged to 6 days, pure plate-like crystals of compound **2** were collected in a yield of about 59% (based on 2-nitrophenylarsonic acid). Its purity was confirmed by powder XRD study (Supporting Information, Figure S1). Elem. anal. calcd (%) for $C_{13}H_8O_9N_3As_2Ag_3$ (M_r = 823.67): C, 18.96; H, 0.98; N, 5.10. Found: C, 19.20; H, 1.13; N, 5.25. IR data for **2** (KBr, cm^{-1}): 3066(w), 2735(m), 2321(m), 2140(w), 1599(m),

dx.doi.org/10.1021/ic301935g | Inorg. Chem. 2013, 52, 1843−1853

Table 2. Important Bond Lengths (Å) for H_2L^4 and Compounds 1−4[a]

	H_2L^4		
As(1)−O(1)	1.636(2)	As(1)−O(3)	1.7588(14)
As(1)−O(2)	1.677(2)	As(1)−C(1)	1.920(3)
N(1)−O(4)	1.220(4)	N(1)−O(5)	1.221(3)
N(1)−C(2)	1.470(4)		
	Compound **1**		
Ag(1)−O(1)	2.236(3)	As(1)−O(1)	1.656(3)
Ag(1)−O(5)#1	2.519(3)	As(1)−O(2)	1.655(3)
Ag(1)−N(1)	2.105(4)	As(1)−O(3)	1.757(3)
Ag(2)−O(2)	2.149(3)	As(2)−O(5)	1.654(3)
Ag(2)−C(13)#2	2.035(5)	As(2)−O(4)	1.661(3)
Ag(3)−O(5)#1	2.248(4)	As(2)−O(3)	1.767(3)
Ag(3)−O(4)	2.334(3)	N(1)−C(13)	1.136(6)
Ag(3)−O(2)#3	2.494(3)		
	Compound **2**		
Ag(1)−C(13)#1	2.124(7)	Ag(3)−N(3)#5	2.479(6)
Ag(1)−O(4)#2	2.284(4)	Ag(1)−Ag(2)#2	2.7674(9)
Ag(1)−O(1)	2.365(5)	As(1)−O(1)	1.637(4)
Ag(1)−O(2)#3	2.505(4)	As(1)−O(2)	1.648(4)
Ag(2)−C(13)#4	2.221(6)	As(1)−O(3)	1.752(5)
Ag(2)−O(2)	2.286(4)	As(2)−O(5)	1.641(4)
Ag(2)−N(3)	2.318(6)	As(2)−O(4)	1.655(4)
Ag(2)−O(4)#5	2.434(5)	As(2)−O(3)	1.757(4)
Ag(3)−O(5)	2.250(5)	N(3)−C(13)	1.145(8)
Ag(3)−O(1)#6	2.254(4)		
	Compound **3**		
Ag(1)−O(1)	2.195(5)	Ag(3)−O(9)	2.291(5)
Ag(1)−O(7)	2.205(5)	Ag(3)−O(2)#4	2.385(5)
Ag(1)−O(8)#1	2.517(5)	As(1)−O(1)	1.684(5)
Ag(1)−O(3)#2	2.524(5)	As(1)−O(2)	1.665(5)
Ag(2)−O(2)#1	2.271(5)	As(1)−O(3)	1.721(5)
Ag(2)−O(8)#3	2.381(5)	As(2)−O(7)	1.679(5)
Ag(2)−O(7)	2.444(5)	As(2)−O(8)	1.672(5)
Ag(2)−O(8)#1	2.470(5)	As(2)−O(9)	1.709(5)
Ag(3)−O(1)#2	2.221(5)		
	Compound **4**		
Ag(1)−O(3)	2.175(12)	Ag(4)−O(1)#3	2.195(11)
Ag(1)−O(7)#1	2.230(10)	Ag(4)−O(8)#2	2.209(10)
Ag(1)−O(2)#2	2.468(12)	Ag(4)−O(9)	2.410(13)
Ag(2)−O(3)	2.262(12)	Ag(4)−O(7)#1	2.508(11)
Ag(2)−O(9)#3	2.292(11)	As(1)−O(1)	1.682(11)
Ag(2)−O(2)#3	2.411(13)	As(1)−O(2)	1.664(12)
Ag(2)−O(1)#2	2.492(12)	As(1)−O(3)	1.671(14)
Ag(3)−O(8)#1	2.166(11)	As(2)−O(7)	1.670(10)
Ag(3)−O(2)	2.213(11)	As(2)−O(8)	1.677(13)
Ag(3)−O(7)#4	2.414(12)	As(2)−O(9)	1.656(11)

[a]Symmetry transformations used to generate equivalent atoms: For **1**: #1, −*x*+1, −*y*, −*z*+1; #2, −*x*, −*y*−1, −*z*+1; #3, −*x*, −*y*, −*z*+1. For **2**: #1, *x*, −*y*+1/2, *z*−1/2; #2, *x*, *y*, *z*−1; #3, −*x*+2, −*y*, −*z*+1; #4, *x*, −*y*+1/2, *z*+1/2; #5, −*x*+2, −*y*, −*z*+2; #6, *x*, −*y*−1/2, *z*+1/2. For **3**: #1, −*x*, −*y*, −*z*+1; #2, −*x*, −*y*+1, −*z*+1; #3, *x*+1, *y*, *z*; #4, −*x*−1, −*y*+1, −*z*+1. For **4**: #1, −*x*+1, *y*+1/2, −*z*; #2, *x*, *y*+1, *z*; #3, −*x*+2, *y*+1/2, −*z*; #4, −*x*+1, *y*−1/2, −*z*.

1530(s), 1430(w), 1347(s), 1295(m), 1167(w), 1114(m), 1053(w), 918(s), 864(s), 826(m), 789(m), 747(m), 688(w), 484(w), 419(w).

Synthesis of $[Ag_3(HL^5)(H_2L^5)]$ (3). A mixture of $Ag(CH_3COO)$ (0.3 mmol) and 4-hydroxy-3-nitrophenylarsonic acid (0.2 mmol) in 3 mL of acetonitrile was sealed to a Parr Teflon-lined autoclave (23 mL) and heated at 100 °C for 4 days. Yellow plate-like crystals were recovered in about 84% yield (based on 4-hydroxy-3-nitrophenylarsonic acid). Its purity was confirmed by powder XRD (Supporting Information, Figure S1). Elem. anal. calcd (%) for $C_{12}H_9O_{12}N_2As_2Ag_3$ (M_r = 846.66): C, 17.02; H, 1.07; N, 3.31. Found: C, 17.27; H, 1.17; N, 3.39. IR data for **3** (KBr, cm^{-1}): 3432(s), 2318(w), 1610(s), 1532(s), 1410(w), 1326(m), 1248(s), 1153(m), 1094(m), 897(w), 832(w), 773(w), 624(w), 546(w).

Synthesis of $[Ag_2(HL^5)]$ (4). A mixture of $Ag(CH_3COO)$ (0.2 mmol) and 4-hydroxy-3-nitrophenylarsonic acid (0.1 mmol) in 2 mL of acetonitrile was sealed to a Parr Teflon-lined autoclave (23 mL) and heated at 100 °C for 4 days. Very thin plate-like crystals of **4** were recovered in about 73% yield (based on 4-hydroxy-3-nitrophenylarsonic acid). It is worthy to note that when the reaction temperature was raised to 120 °C, compound **3** will be obtained. The purity of **4** was confirmed by powder XRD studies (Supporting Information, Figure S1). Elem. anal. calcd (%) for $C_{12}H_8O_{12}N_2As_2Ag_4$ (M_r = 953.52): C, 15.12; H, 0.84; N, 2.94. Found: C, 15.28; H, 0.97; N, 2.97. IR data for **4** (KBr, cm^{-1}): 3412(vs), 2920(w), 2323(w), 1610(s), 1542(m), 1442(w), 1363(w), 1334(m), 1262(s), 1152(m), 1095(w), 903(w), 874(w), 832(m), 714(m), 627(w), 533(w).

X-ray Crystallography. Data collections were performed on either a Rigaku Saturn 724 CCD diffractometer (for **1** and **2**) or a Rigaku Mercury CCD diffractometer (for H_2L^4, **3** and **4**). Both diffractometers were equipped with graphite-monochromated Mo−Kα radiation (λ = 0.71073 Å). Intensity data for all four compounds were collected by the narrow frame method at 293 K. The five data sets were corrected for Lorentz and polarization factors as well as for absorption by the Multiscan method.[15a] All five structures were solved by the direct methods and refined by full-matrix least-squares fitting on F^2 using SHELX-97.[15b] All non-hydrogen atoms were refined with anisotropic thermal parameters except that O6, O9 in complex **2** and O1, O3, O6, O7 in complex **4** were refined with ISOR restraints. Without these restraints, these atoms will be nonpostive-definite when refined anistropically. All hydrogen atoms associated with phenyl ring and hydroxyl groups were located at geometrically calculated positions and refined with isotropic thermal parameters. The structures were also checked for possible missing symmetry with PLATON.[15c] The refined Flack parameter of chiral compound **4** is 0.02(5), indicating the correctness of its absolute structure. The refinements of compound **4** are not so good because of the poor quality of its single crystals with a thin plate shape, though several data sets were collected on several different crystals, results showed little improvement. Crystallographic data and structural refinements for compounds **1**−**4** as well as H_2L^4 are summarized in Table 1. Important bond lengths are listed in Table 2. More details on the crystallographic studies are given as Supporting Information.

RESULTS AND DISCUSSION

Compounds **1**−**4** have been synthesized in acetonitrile under solvothermal condition. They represent the first structurally characterized Ag(I) arsonates. For compounds **1** and **2**, the new arsonate ligands with As−O−As linkages were formed by condensation of two corresponding arsonate ligands with the release of one mole of water (Scheme 1). It is noted that the

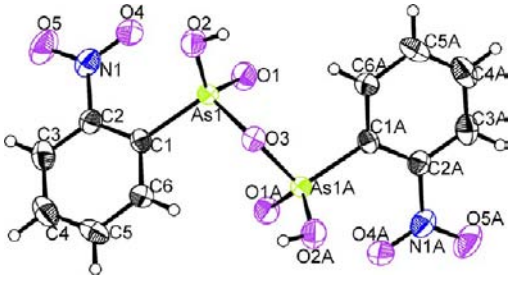

Figure 1. View of H_2L^4 with 50% probability displacement ellipsoids. H atoms are shown as small spheres of arbitrary radii. Symmetry codes for the generated atoms: (a) −*x*, *y*, −*z* + 3/2.

dx.doi.org/10.1021/ic301935g | Inorg. Chem. 2013, 52, 1843−1853

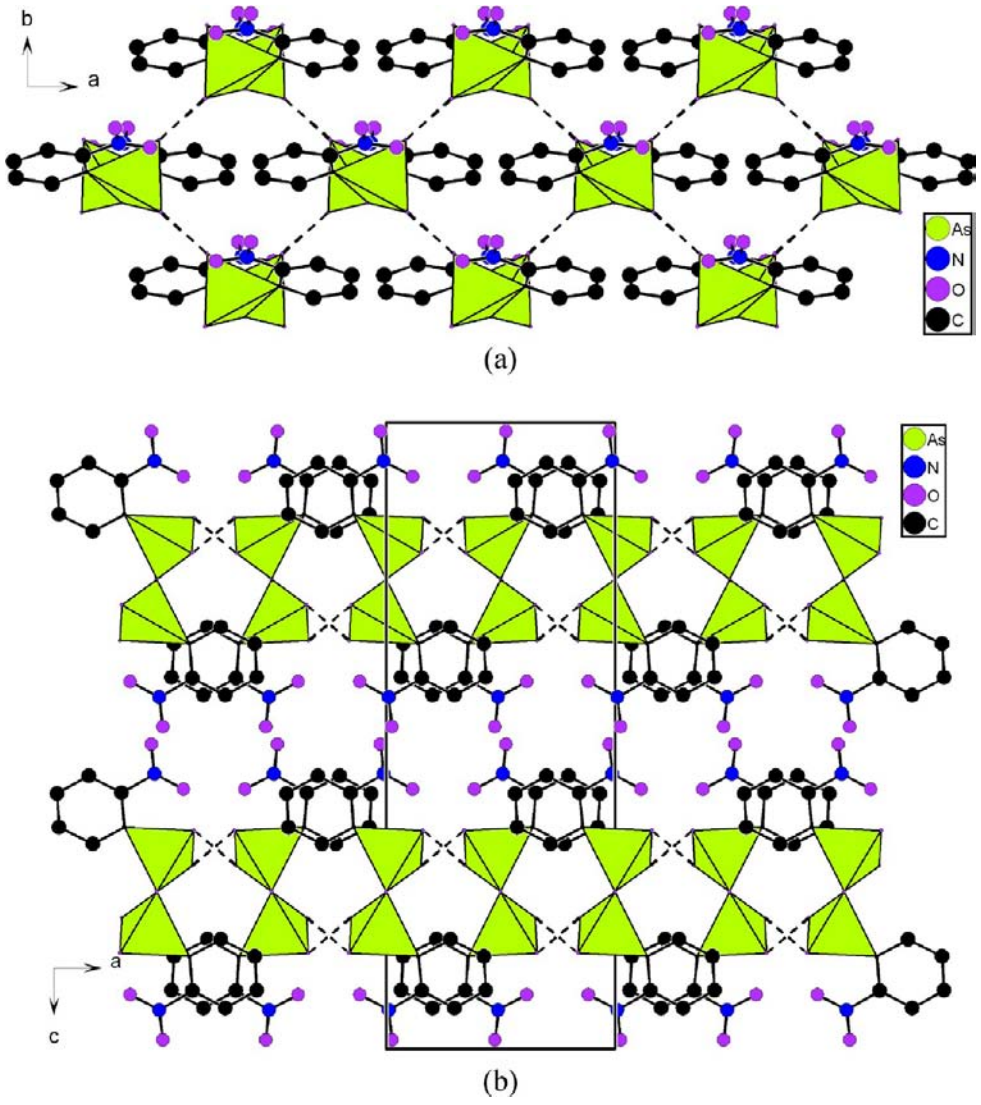

Figure 2. View of the 2D layered hydrogen bonding network of H_2L^4 (a) and the packing structure of H_2L^4 along *b* axis (b). The hydrogen bonding interactions are represented by dashed lines.

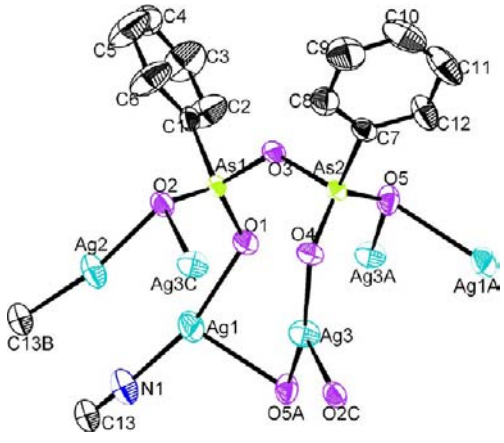

Figure 3. ORTEP representation of the selected unit in compound **1**. The thermal ellipsoids are drawn at 50% probability level. Symmetry codes for the generated atoms: (a) $-x+1, -y, -z+1$; (b) $-x, -y-1, -z+1$; (c) $-x, -y, -z+1$.

reaction of phenylarsonic acid (or 2-nitrophenylarsonic acid) alone under the same condition yields no species with As−O−As linkage, the reaction of phenylarsonic acid (or 2-nitrophenylarsonic acid) in the presence of small amounts of $AgNO_3$ produced the condensed product, confirming that the polyarsonate ligands were formed in a metal-mediated thermally induced process. Furthermore, the CN^- anions in compounds **1** and **2** formed by in situ decomposition of the acetonitrile molecules. A similar process had been reported during the preparation of the metal pyrophosphonates.[16,17] So far, only two examples of metal pyroarsonates have been reported in the literature.[18]

Syntheses. The reaction conditions for complexes **1**−**4** have been listed in Supporting Information, Table S1. Additional experiments have been also performed to explore the effects of Ag^+ source, the amount of acetonitrile, temperature, and reaction time on the compositions and structures of the final products formed.

For **1**, when $Ag(CH_3COO)$ was used as the Ag^+ source, crystals of **1** can be isolated along with a lot of black impurities. Using $AgNO_3$ as the Ag^+ source led to the isolation of the pure phase of **1**. It is also found that elongation of the reaction time helps to enhance the yield. **2** can be synthesized under shorter reaction time, lower temperature, and higher yield compared

dx.doi.org/10.1021/ic301935g | *Inorg. Chem.* 2013, 52, 1843−1853

Scheme 2. Coordination Modes of the Ligands in Compounds 1(a), 2(b), 3(c), and 4(d)

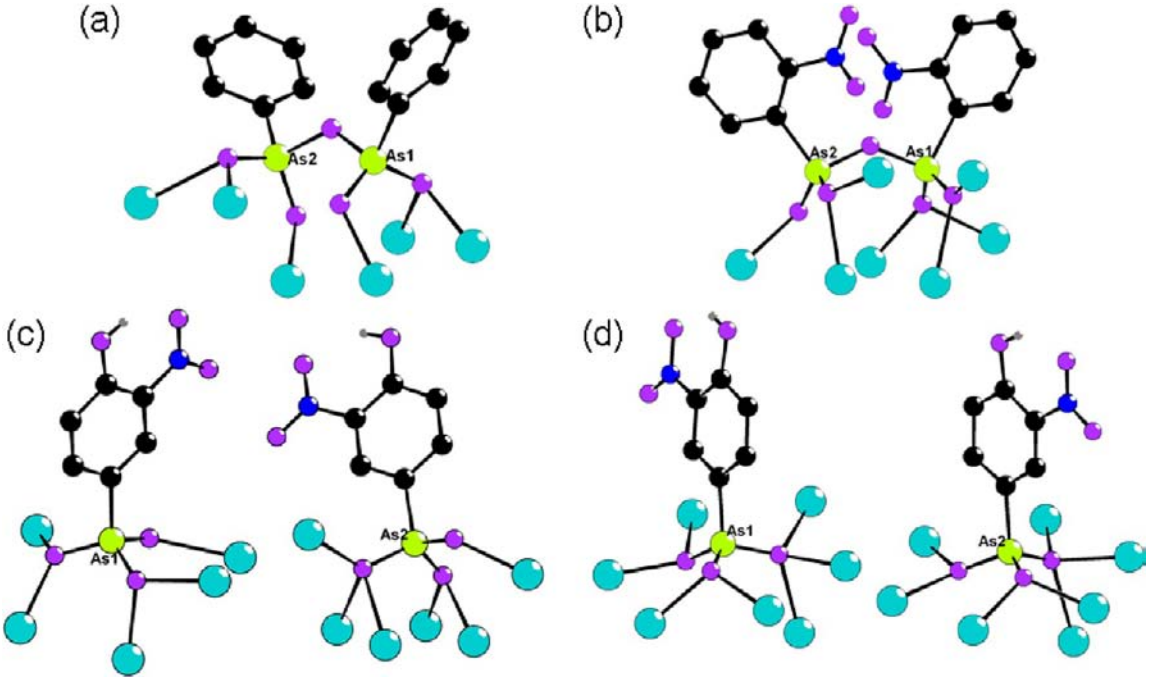

with those of **1**. When $Ag(CH_3COO)$ was used as Ag^+ source, the crystals of **2** could not be isolated. For the syntheses of **3** and **4**, the metal/ligand molar ratios applied and reaction temperatures are important. At 100 °C, when the metal/ligand molar ratio is 3:2, the resulting product will be **3**; when the metal/ligand molar ratio is 2:1, the resulting product will be **4**. At a higher reaction temperature of 120 °C, **3** will be obtained regardless if the $Ag(CH_3COO)/H_3L^5$ molar ratio is 3:2 or 2:1. The amount of acetonitrile added affects the yield and morphology of the crystals of **3**. When $AgNO_3$ was used as Ag^+ source in these reactions, only unknown red-brown power was obtained. According to our experiments, it is best to control the amount of acetonitrile to be 2−3 mL for all four complexes.

It is also interesting to note that the condensation reactions of the arsonate ligands occurred for **1** and **2** but not for **3** and **4**. We suspect it may be due to the number and nature of the substituents on the benzene rings of the arsonate ligands. The $Ph\text{-}AsO_3H_2$ has only one $\text{-}AsO_3$ group on its benzene ring and $2\text{-}NO_2\text{-}C_6H_4\text{-}AsO_3H_2$ contains an additional *ortho*-nitro group whereas the benzene ring of $3\text{-}NO_2\text{-}4\text{-}OH\text{-}C_6H_3\text{-}AsO_3H_2$ contains additional *meta*-nitro and *para*-OH groups. It is known that the nitro group is electron withdrawing whereas the hydroxyl group is electron donating. Furthermore the nitro group on the ortho-position can withdraw eletrons more effectively than that of meta-position. An electron withdrawing group will enhance the reactivity of the organic ligand whereas an electron donating group lowered the reactivity of an organic ligand. Hence the reactivities of the three arsonate ligands have the following order: $2\text{-}NO_2\text{-}C_6H_4\text{-}AsO_3H_2$ > $Ph\text{-}AsO_3H_2$ > $3\text{-}NO_2\text{-}4\text{-}OH\text{-}C_6H_3\text{-}AsO_3H_2$. Therefore the condensation reaction for $3\text{-}NO_2\text{-}4\text{-}OH\text{-}C_6H_3\text{-}AsO_3H_2$ does not occur easily.

Structure of H_2L^4. H_2L^4 crystallizes in the orthorhombic space group *Pbcn*, and its crystal structure features a 2D hydrogen bonded supramolecular sheet. Its asymmetric unit contains half of the H_2L^4 molecule (Figure 1). The As−O distances range from 1.632(2) to 1.759(2) Å. The As−O distance of the As−O(3)−As bridge is significantly larger than those of the four terminal As−O bonds. O(2) is protonated hence As(1)−O(2) is significantly longer than that of As(1)−O(1). As shown in Figure 2, each independent H_2L^4 unit connects with 4 neighboring H_2L^4 molecules through strong O−H···O hydrogen bonds (Supporting Information, Table S2) to form a 2D sheet (Figure 2a). The interlayer distance is close to 11.6 Å (half of the *c*-axis). These 2D layers are further cross-linked by weak $\pi\cdots\pi$ interactions between the phenyl rings (Figure 2b).

Structure of $[Ag_3(L^3)(CN)]$ (1). Compound **1** crystallizes in the triclinic space group $P\bar{1}$ and features a 2D wave-like layer parallel to the *ab* plane. Its asymmetric unit consists of three Ag(I) ions, one $\{L^3\}^{2-}$ and one CN^- anions. As shown in Figure 3, Ag1 is three-coordinated by two arsonate oxygen atoms from two different $\{L^3\}^{2-}$ anions, and one nitrogen atom from a CN^- anion. Ag2 is two-coordinated by one arsonate oxygen atom and one carbon atom from a CN^- anion. Ag3 is three-coordinated by three arsonate oxygen atoms from three different $\{L^3\}^{2-}$ anions. Both Ag1 and Ag3 are in a trigonal coordination geometry. The Ag−O distances are in the range of 2.149(3)−2.519(3) Å, which are comparable to those reported in Ag(I) phosphonates.[16,19] Each $\{L^3\}^{2-}$ anion connects six Ag(I) ions. O2 and O5 are bidentate bridging whereas O1 and O4 is unidentate, O3 forms a As−O−As bridge and it is not coordinated to the silver ion (Scheme 2a). Each CN^- anion bridges two Ag(I) ions by using its nitrogen and carbon atoms, with the angles of Ag1−C−N and C−N−Ag2 of 173.7(4)° and 172.7(5)°, respectively. The Ag1−C−N−Ag2 is almost in a straight line.

The interconnection of Ag(I) ions by chelating $\{L^3\}^{2-}$ anions resulted in an infinite chain along the *a* axis. Within the 1D chain, six coplanar Ag(I) ions are bridged by two arsonate ligands into a hexanuclear cluster unit with moderate Ag···Ag interactions [3.144(1)−3.262(1) Å] (Figure 4a). Neighboring 1D chains are further interconnected by CN^- anions via the coordination of the nitrogen and carbon atoms with the Ag(I)

dx.doi.org/10.1021/ic301935g | Inorg. Chem. 2013, 52, 1843−1853

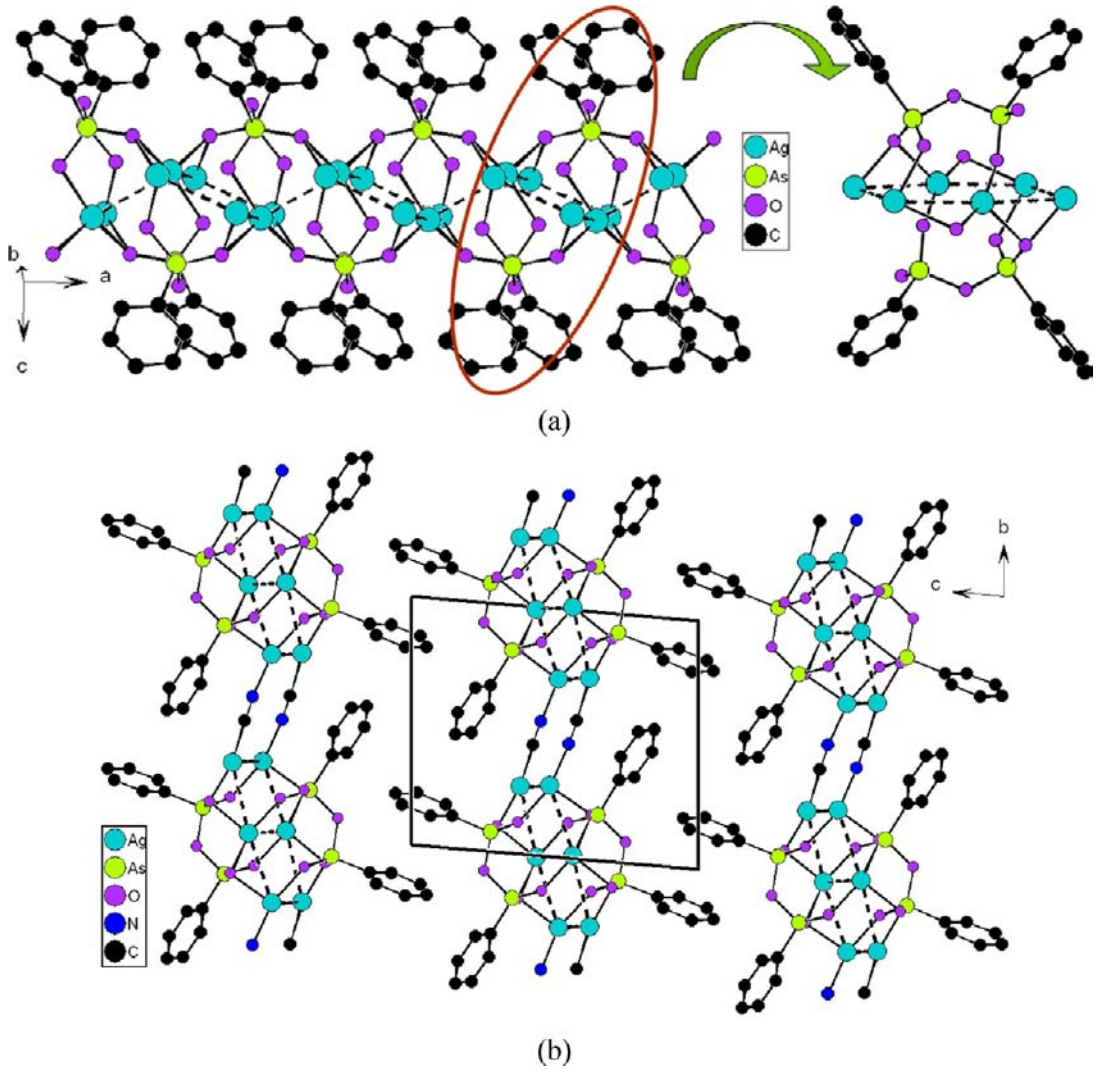

Figure 4. View of the infinite chain of Ag(I) ions by chelating $\{L^3\}^{2-}$ anions and a six-membered ring of Ag(I) ions in one plane within the chain (a), and the packing structure of **1** along *a* axis (b). All H atoms are omitted for clarity.

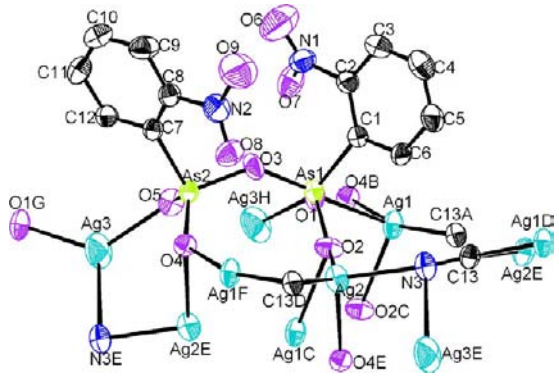

Figure 5. ORTEP representation of the selected unit in compound **2**. The thermal ellipsoids are drawn at 50% probability level. Symmetry codes for the generated atoms: (a) *x*, −*y*+1/2, *z*−1/2; (b) *x*, *y*, *z*−1; (c) −*x*+2, −*y*, −*z*+1; (d) *x*, −*y*+1/2, *z*+1/2; (e) −*x*+2, −*y*, −*z*+2; (f) *x*, *y*, *z*+1; (g) *x*, −*y*−1/2, *z*+1/2; (h) *x*, −*y*−1/2, *z*−1/2.

ions from neighboring chains into a wave-like layer with the phenyl groups orientated toward the interlayer space (Figure 4b).

Structure of $[Ag_3(L^4)(CN)]$ (2). Compound **2** crystallizes in the monoclinic space group $P2_1/c$ and features a 2D wave-like layer paralell to the *bc* plane. Its asymmetric unit consists of three Ag(I) ions, one $\{L^4\}^{2-}$ and one CN^- anions. As shown in Figure 5, Ag1 is four-coordinated by three arsonate oxygen atoms from three different $\{L^4\}^{2-}$ anions, and one carbon atom from a CN^- anion. Ag2 is four-coordinated by two arsonate oxygen atoms from two $\{L^4\}^{2-}$ anions, one carbon and one nitrogen atom from two different CN^- anions. Ag3 is three-coordinated by two arsonate oxygen atoms from two different $\{L^4\}^{2-}$ anions and one nitrogen atom from a CN^- anion. Ag1 and Ag2 adopt distorted tetrahedral geometry whereas Ag3 adopts a trigonal geometry. The Ag−O, Ag−N, and Ag−C bond distances are in the ranges of 2.250(5)−2.505(4) Å, 2.318(6)−2.479(6) Å, and 2.124(7)−2.221(6) Å, respectively. Each $\{L^4\}^{2-}$ anion connects 7 Ag(I) ions. Three of the arsonate oxygens, O1, O2, and O4, are bidentate and each bridges with two Ag(I) ions. O5 is unidentate and bonds with a Ag(I) ion whereas O3 of the As−O−As involves no metal coordination (Scheme 2b). The coordination mode of CN^- is very different from that of compound **1**. Each CN^- anion bridges with four Ag(I) ions, both nitrogen and carbon atoms are bidentate.

dx.doi.org/10.1021/ic301935g | *Inorg. Chem.* 2013, 52, 1843−1853

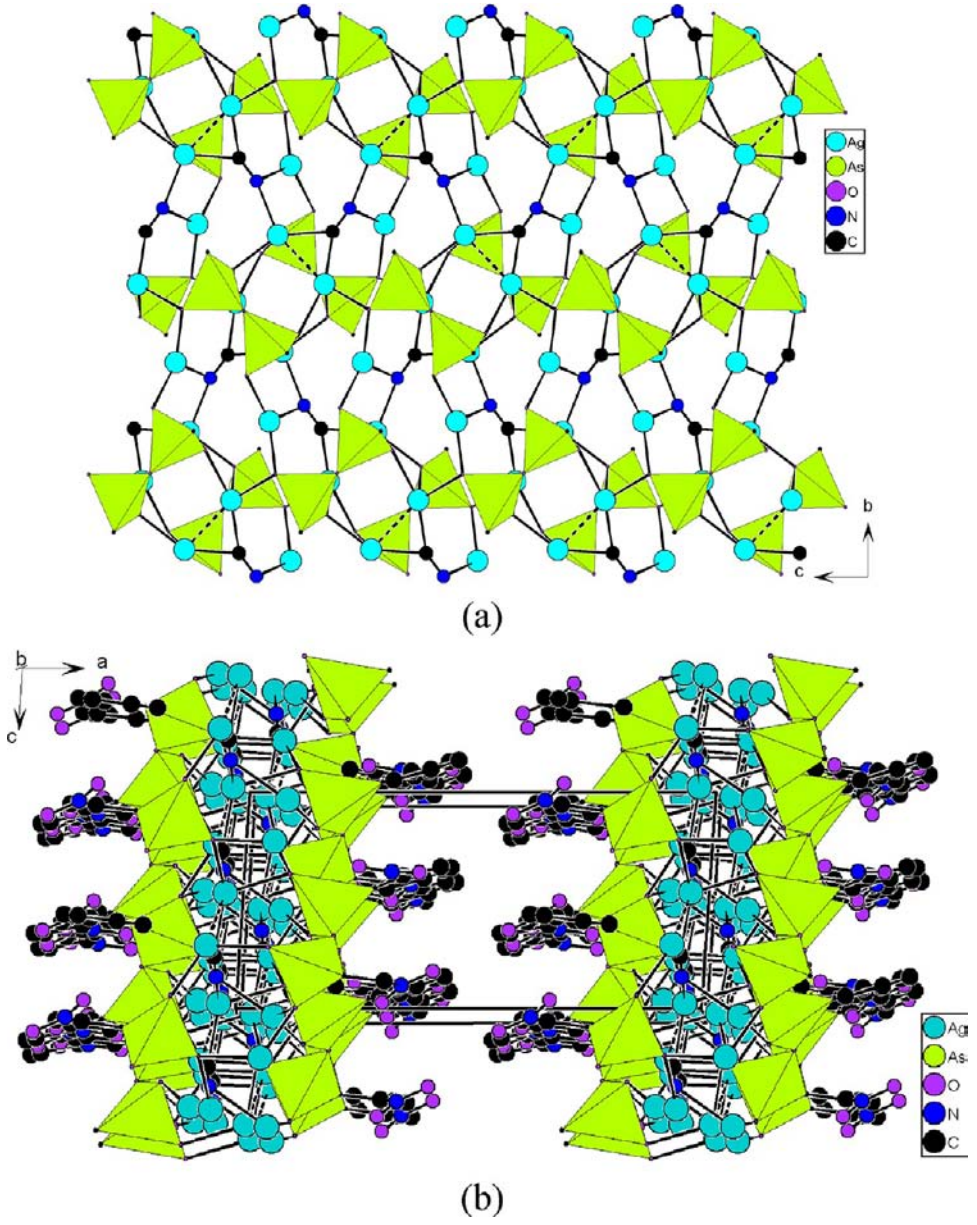

Figure 6. View of the 2D hybrid layer of **2** paralell to the *bc* plane (a), the packing structure of **2** along *b* axis (b). All H atoms are omitted for clarity.

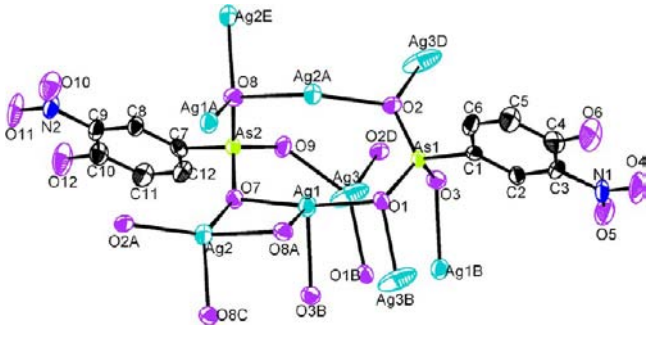

Figure 7. ORTEP representation of the selected unit in compound **3**. The thermal ellipsoids are drawn at 50% probability level. Symmetry codes for the generated atoms: (a) $-x, -y, -z+1$; (b) $-x, -y+1, -z+1$; (c) $x+1, y, z$; (d) $-x-1, -y+1, -z+1$; (e) $x-1, y, z$.

The Ag(I) ions are interconnected by bridging $\{L^4\}^{2-}$ and CN^- anions into a complicated 2D hybrid layer paralell to the *bc* plane. The interconnection of the Ag(I) ions by bridging $\{L^4\}^{2-}$ anions form the main skeleton of the layer with Ag_3As_3 rings which are filled by the CN^- anions (Figure 6a). The Ag···Ag contact of 2.7674(9) Å for the Ag−C−Ag bridge is significantly shorter than the Ag···Ag separation of 2.88 Å in the metallic state.[20] The overall structure can be described as wave-like layers stacking along the *a* axis, with the phenyl groups and noncoordination nitro groups oriented toward the interlayer space (Figure 6b).

Structure of $[Ag_3(HL^5)(H_2L^5)]$ (3). The structure of **3** features a Ag(I) arsonate 2D layer. As shown in Figure 7, its asymmetric unit consists of three Ag(I) ions, one $\{HL^5\}^{2-}$, and one $\{H_2L^5\}^-$ anions. Ag1 is four-coordinated by four arsonate oxygen atoms from two $\{HL^5\}^{2-}$ and two $\{H_2L^5\}^-$ anions whereas Ag2 is four-coordinated by four arsonate oxygen atoms from three $\{HL^5\}^{2-}$ and one $\{H_2L^5\}^-$ anions, and Ag3 is three-coordinated by three arsonate oxygen atoms from two $\{HL^5\}^{2-}$ and one $\{H_2L^5\}^-$ anions. The Ag−O distances are in the range of 2.195(5)−2.524(5) Å, which are comparable to those

dx.doi.org/10.1021/ic301935g | *Inorg. Chem.* 2013, 52, 1843−1853

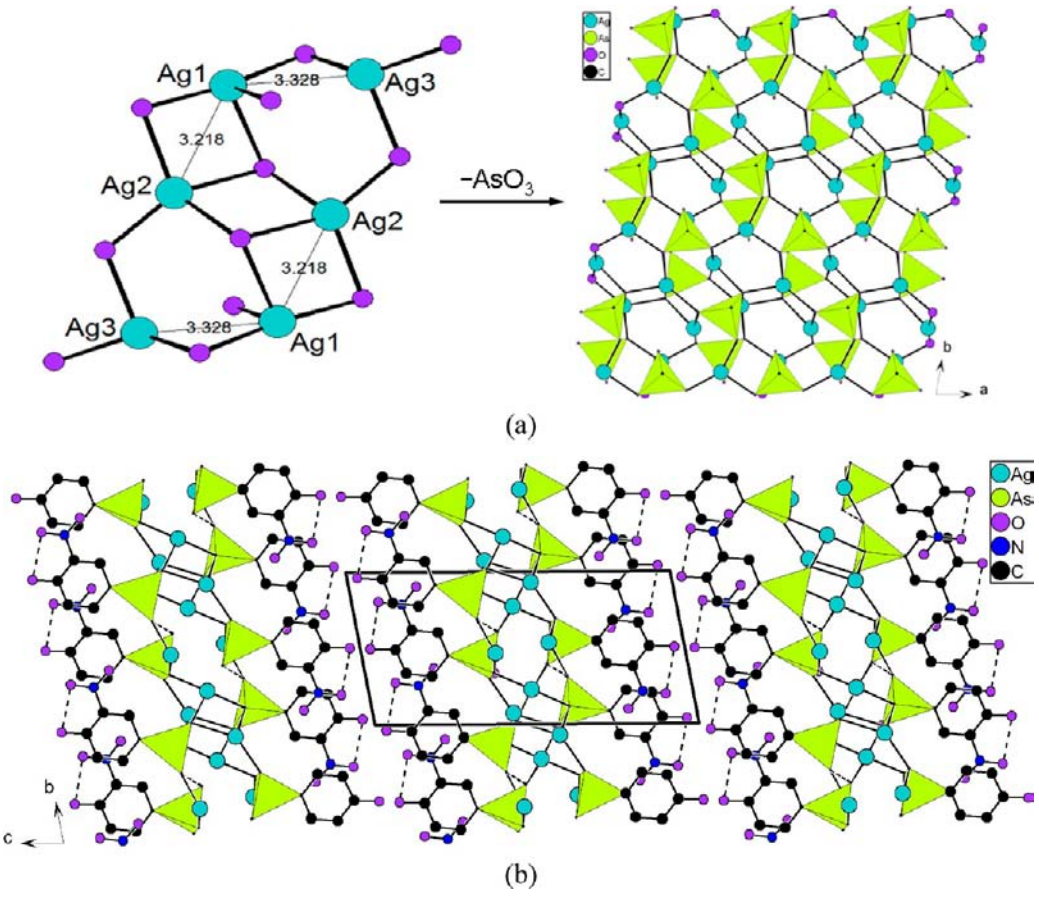

Figure 8. View of the hexanuclear $\{Ag_6O_{12}\}$ clusters interconnected by bridging arsonic groups into a silver(I) arsonate hybrid layer in compound **3** (a), view of the packing structure of **3** along *a* axis (b). All H atoms are omitted for clarity.

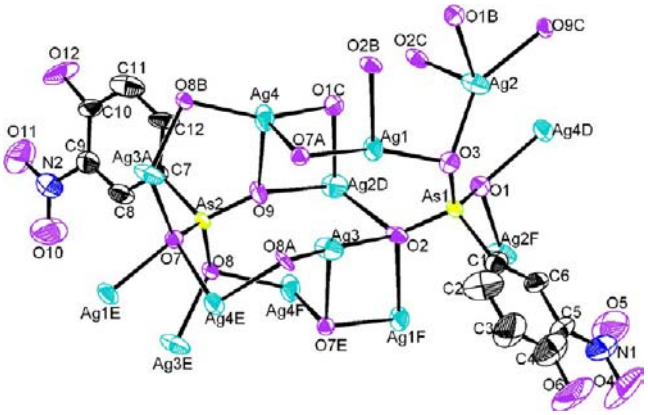

Figure 9. ORTEP representation of the selected unit in compound **4**. The thermal ellipsoids are drawn at 50% probability level. Symmetry codes for the generated atoms: (a) $-x+1, y+1/2, -z$; (b) $x, y+1, z$; (c) $-x+2, y+1/2, -z$; (d) $-x+2, y-1/2, -z$; (e) $-x+1, y-1/2, -z$; (f) $x, y-1, z$.

reported in Ag(I) phosphonates.[19] The two arsonate ligands are different in charge and coordination mode. The $\{HL^5\}^{2-}$ anion containing As(2) is −2 in charge whereas the $\{H_2L^5\}^-$ anion containing As(1) is −1 in charge. The O3 atom is protonated and exhibits a longer As−O distance. Both $\{HL^5\}^{2-}$ and $\{H_2L^5\}^-$ anions contain a hydroxyl group on the phenyl ring. The $\{H_2L^5\}^-$ anion is pentadentate, O1 and O2 are bidentate bridging, and the protonated O3 is monodentate. The $\{HL^5\}^{2-}$, anion acts as hexadentate metal linker, O7, O8, and O9 bridge with two, three, and one Ag(I) ions, respectively (Scheme 2c).

As shown in Figure 8a, the three types of Ag(I) ions are interconnected by bridging arsonate oxygens, resulting in the formation of hexanuclear $\{Ag_6O_{12}\}$ clusters. Such hexanuclear clusters are further interconnected by arsonate groups into a 2D silver(I) arsonate layer. The organic groups are orientated toward the interlayer space (Figure 8b). Intralayer hydrogen bonds are formed between the −OH and $-NO_2$ groups in both $\{HL^5\}^{2-}$ and $\{H_2L^5\}^-$ anions (Supporting Information, Table S2).

Structure of $[Ag_2(HL^5)]$ (4). Compound **4** crystallizes in the monoclinic space group $P2_1$ and features a Ag(I) arsonate layer as well. The structure of **4** differs significantly from that of compound **3**. As shown in Figure 9, there are four different Ag(I) atoms in each asymmetric unit. Both Ag1 and Ag3 are three-coordinated by three arsonate oxygen atoms from three different $\{HL^5\}^{2-}$ anions, adopting trigonal geometries, whereas Ag2 and Ag4 are four-coordinated by four different $\{HL^5\}^{2-}$ anions in a distorted tetrahedral geometry. The Ag−O distances are in the range of 2.18(1)−2.49(1) Å. There are two $\{HL^5\}^{2-}$ anions in each asymmetric unit. Both of them bridge with seven Ag(I) ions, two of the arsonate oxygens are bidentate whereas the third one is tridentate (Scheme 2d). The hydroxyl and nitro groups are not involved in metal coordination.

The Ag(I) ions are interconnected by bidentately and tridentately bridging arsonate oxygens into right-handed $\{Ag_4O_4\}$ chains. These chains are further interconnected by

dx.doi.org/10.1021/ic301935g | Inorg. Chem. 2013, 52, 1843−1853

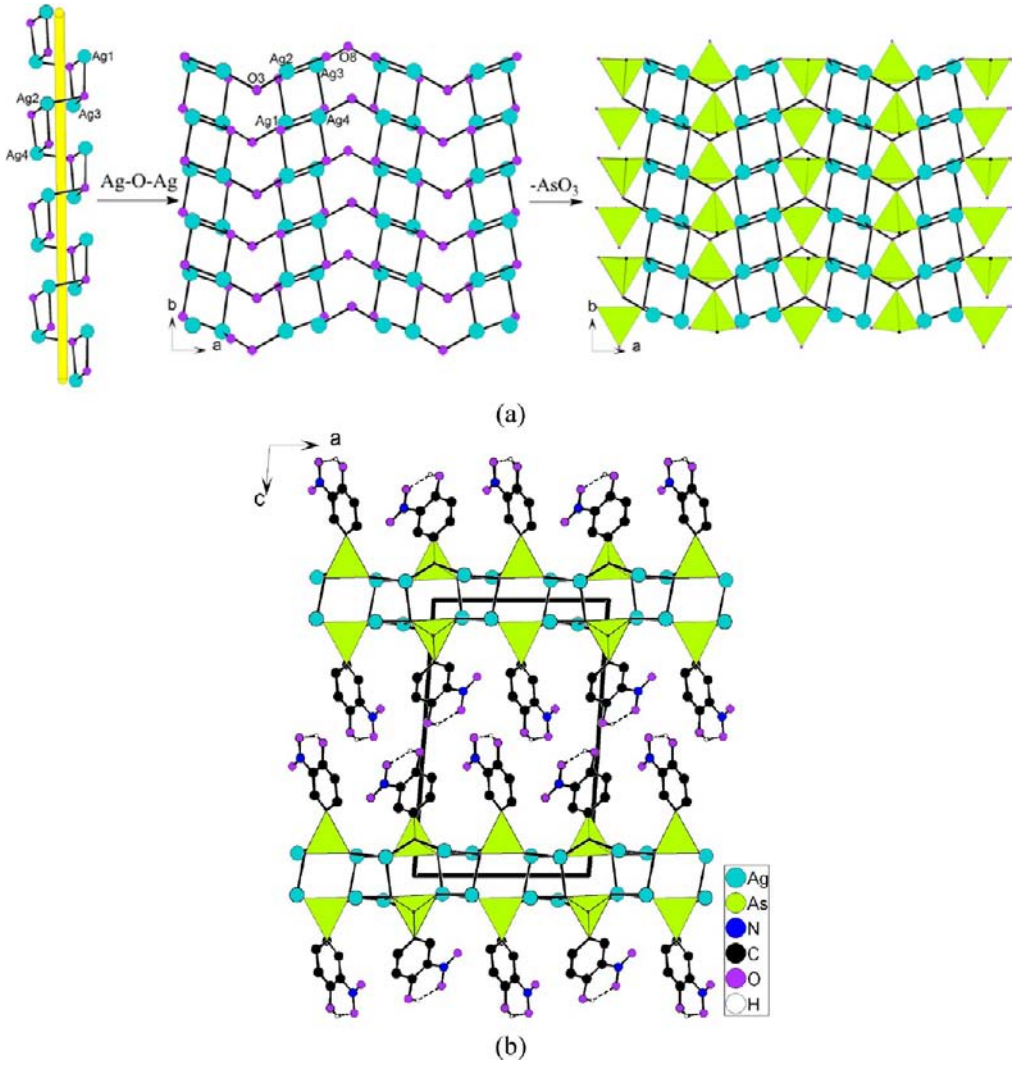

Figure 10. View of the right-handed $\{Ag_4O_4\}$ chains interconnected by Ag−O−Ag bridges and arsonate ligands into a silver(I) arsonate layer in compound **4** (a), a view of the layers of **4** stacking along *b* axis (b).

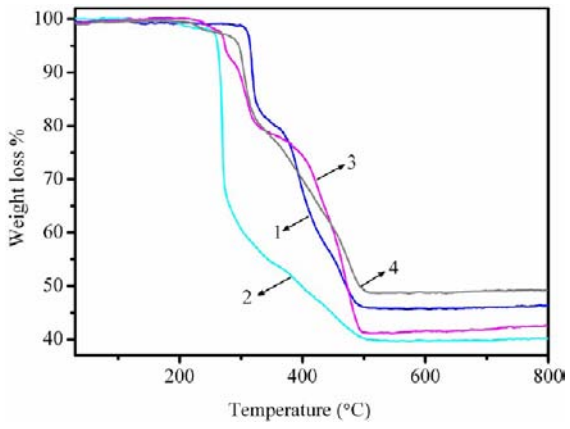

Figure 11. TGA curves for compounds **1**−**4**.

organoarsonate ligands as well as additional Ag−O−Ag bridges into novel silver(I) arsonate layers (Figure 10a). The phenyl groups, hydroxyl and nitro substitute groups on the phenyl rings of the arsonate ligands are oriented toward the interlayer region. Unlike the paralell arrangements in compound **3**, these phenyl groups in compound **4** are not paralell to each other, but form a dihedral angle of 52.5°. Similar to that in compound **3**, an intra ligand hydrogen bond is formed between hydroxyl and nitro groups (Figure 10b).

TGA Study. The thermal gravimetric analyses (TGA) of compounds **1**−**4** were carried out at a heating rate of 10 °C/min under an air atmosphere (Figure 11). Compound **1** is stable to about 280 °C, then it exhibits two main steps of weight losses, corresponding to the combustion of organo arsonate and CN^- ligands. Compounds **2**−**4** exhibit a small weight loss before 210 °C, which is probably attributed to the release of the small amount of surface water present in the samples. Compound **2** exhibits a very rapid weight loss from 250 to 500 °C, which corresponds to the combustion of $\{L^4\}^{2-}$ and CN^- ligands. The decomposition profiles for **3** and **4** are similar in the 280−800 °C region, consisting of two main weight losses attributed to the decomposition of organo arsonate ligands. Compounds **1**−**4** exhibit the final plateau almost at the same temperature of about 500 °C, and all the final residues shine with a metallic luster. These residues are assumed to be silver metal, and the observed weights of final products (45.8% for **1**, 40% for **2**, 41.3% for **3** and 48.9% for **4**) are close to the calculated values (44.1% for **1**, 39.8% for **2**, 38.2% for **3**, and 45.3% for **4**).

dx.doi.org/10.1021/ic301935g | *Inorg. Chem.* 2013, 52, 1843−1853

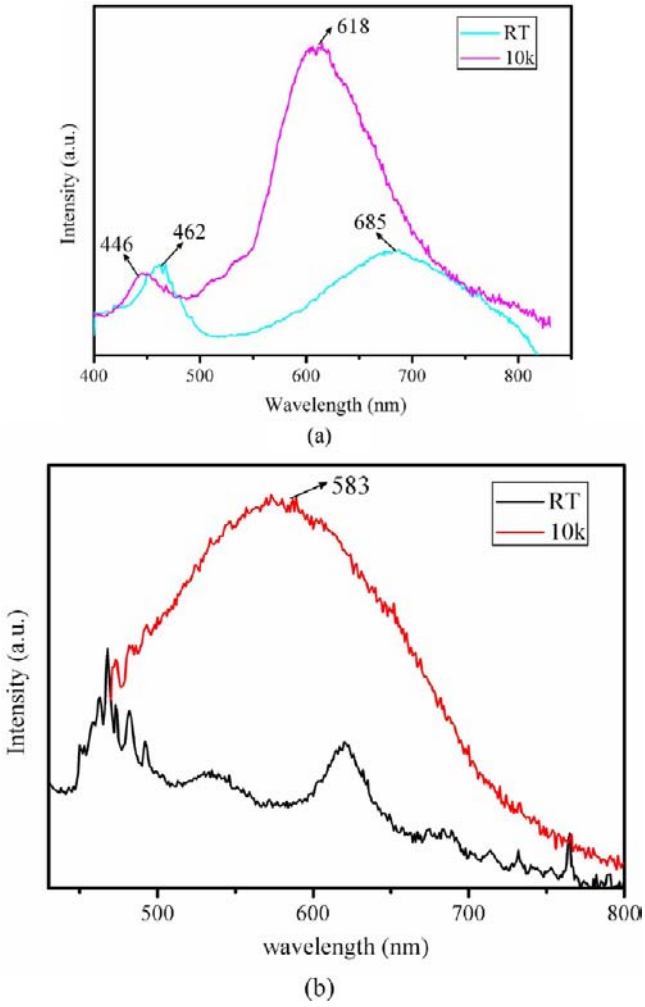

Figure 12. Solid-state emission spectra of compounds **1** (a) and **2** (b) at 10 K and RT.

Luminescent Properties. The solid-state photoluminescent spectra of compounds **1**−**4** as well as the free ligands were measured at room temperature (RT) and 10 K. Compound **1** exhibits a sharp red light emission band at 618 nm and a weak peak at 446 nm (λ_{ex} = 372 nm) at 10 K, and compound **2** displays a broad orange-red light emission band at 583 nm (λ_{ex} = 434 nm) at 10 K (Figure 12b). The luminescences for **3** and **4** are too weak to be observed. The solid-state lifetimes are 9 and 0.5 ns, respectively for **1** and **2**, suggestive of their fluorescent characters. Compared with the emission of free phenylarsonic acid (λ_{ex} = 280 nm, λ_{em} = 475 nm) and 2-nitrophenylarsonic acid (no obvious luminescence) in the solid state at 10 K, the luminescence of **1** and **2** can be attributed to the Ag(I) cluster-based centers therein.[14,21,22] Given the oxidizing nature of Ag(I), a approprite assignment for the origin of the emission involves excited states derived from ligand-to-metal charge transfer (LMCT) transitions mixed with d-s/d-p character. Furthermore, the shortest Ag(I)···Ag(I) distance in **1** is 3.144(1) Å and only 2.7674(9) Å in **2**, which indicate strong Ag(I)···Ag(I) interactions. Since the luminescence of d^{10} systems has a demonstrated sensitivity to metal−metal interactions, the existence of Ag(I)···Ag(I) interactions is expected to play a role in the solid state emission, which are likely responsible for the low energies of the luminescence bands of compounds **1** and **2**.[14,22b,23] In addition, it is noteworthy that the luminescence intensity of compound **1** is much stronger than that of **2** (Complex **2** exhibits no emission at RT.) and a band with higher emission energy is observed for **2**. This may be mainly attributed to the substituent of -NO_2 in compound **2**, which results in a smaller π-conjugated system in the ligand and a larger gap between the highest occupied molecular orbital (HOMO) and the lowest unoccupied molecular orbital (LUMO).[24]

More interestly, **1** shows a temperature-dependent emission. Upon cooling to 10 K, a blue shift of 16 nm for the higher-energy (HE) emission and a blue shift of 67 nm for the lower-energy (LE) emission are observed compared with those measured at RT (Figure 12a). The excitation maximum remains almost unchanged during cooling (375 nm at RT and 372 nm at 10 K). Similar blue shifts of emissions at low temperature have been found in other d^{10} transition metal complexes.[25a−d] It has been reported that the slight distortion of coordination geometry of the central metal ions and shrinkage of the unit cell at low temperatures might cause significant changes for the emission bands (blue shift or red shift).[25b−f] In the absence of crystallographic data for **1** at 10 K, we can only assume that in complex **1**, the blue shifts of these emissions may result from the distortion of the coordination geometry of Ag(I) ions and the slight changes in the average geometry of the complex during cooling. In addition, the enhancement of emission is found to be more obvious in the LE emission band than that in the HE one at 10 K. The HE emission appears to depend on the ligand being π-unsaturated while the more intense LE band originates from the Ag(I) cluster-based centers. As temperature decreased, the rigidity of the ligands should be enhanced,[25b,c] thereby the radiationless decay of the intraligand ($\pi\cdots\pi^*$) excited state is reduced and the delocalization of electron transitions increases. As a result, the LMCT in complex **1** becomes more efficient at low temperature and then the LE emission is much more enhanced than that of the HE emission.

■ CONCLUSIONS

In summary, four new types of Ag(I)-mediated organoarsonates were obtained under solvothermal conditions. The structures of compounds **1**−**2** were constructed by in situ generated $\{RAsO_2(O)O_2AsR\}^{2-}$ and CN^- anions, indicating the occurrence of in situ C−C bond cleavages of the acetonitrile molecules. Both **1** and **2** feature a 2D wave-like layer with short Ag(I)···Ag(I) contacts. Compounds **3** and **4** feature a Ag(I) arsonate 2D layer as well, but compound **4** results in a chiral generation. Complexes **1**−**2** display unusual photoluminescent properties in the red/orange-red region at the low temperature of 10 K, which may be assigned to be an admixture of LMCT and metal-centered (4d-5s/5p) transitions perturbed by Ag(I)···Ag(I) interactions. In addition, upon cooling from RT to 10 K, compound **1** exhibits interesting temperature-dependent emissions. Further work on pyroarsonates generated in situ will continue in our laboratory.

■ ASSOCIATED CONTENT

Ⓢ Supporting Information

X-ray crystallographic files in CIF format, simulated and experimental XRD powder patterns, IR spectra, morphologies and detailed data for hydrogen bonds. This material is available free of charge via the Internet at http://pubs.acs.org.

AUTHOR INFORMATION

Corresponding Author

*E-mail: mjg@fjirsm.ac.cn. Fax: (+86)591-83714946.

Notes

The authors declare no competing financial interest.

ACKNOWLEDGMENTS

This work was supported by the National Natural Science Foundation of China (Nos. 20973170 and 20825104), the major project from FJIRSM (SZD09001).

REFERENCES

(1) (a) Clearfield, A. *Metal Phosphonate Chemistry*; John Wiley & Sons, Inc.: New York, 2007; pp 371−510. (b) Mao, J. G. *Coord. Chem. Rev.* **2007**, *251*, 1493. (c) Matczak-Jon, E.; Videnova-Adrabinska, V. *Coord. Chem. Rev.* **2005**, *249*, 2458. (d) Maeda, K. *Microporous Mesoporous Mater.* **2004**, *73*, 47.

(2) (a) Ngo, H. L.; Lin, W. *J. Am. Chem. Soc.* **2002**, *124*, 14298. (b) Zhu, J.; Bu, X. H.; Feng, P. Y.; Stucky, G. D. *J. Am. Chem. Soc.* **2000**, *122*, 11563. (c) Cheetham, A. K.; Ferey, G.; Loiseau, T. *Angew. Chem., Int. Ed.* **1999**, *38*, 3268. (d) Rao, C. N. R.; Natarajan, S.; Vaidhyanathan, R. *Angew. Chem., Int. Ed.* **2004**, *43*, 1466.

(3) (a) Burkholder, E.; Zubieta, J. *Inorg. Chim. Acta* **2004**, *357*, 301. (b) Burkholder, E.; Wright, E.; Golub, V.; O'Connor, C. J.; Zubieta, J. *Inorg. Chem.* **2003**, *42*, 7460. (c) Barkigia, K. M.; Rajkovic-Blazer, L. M.; Pope, M. T.; Quicksall, C. O. *Inorg. Chem.* **1981**, *20*, 3318. (d) Johnson, B. J. S.; Geers, S. A.; Brennessel, W. W.; Young, V. G.; Stein, A. *Dalton Trans.* **2003**, 4678. (e) Liu, B.; Ku, Y.; Wang, M.; Zheng, P. *Inorg. Chem.* **1988**, *27*, 3868.

(4) (a) Matsumoto, K. Y. *Bull. Chem. Soc. Jpn.* **1978**, *51*, 492. (b) Liu, B. Y.; Xie, G. Y.; Ku, Y. T.; Wang, X. *Polyhedron* **1990**, *9*, 2023. (c) Khan, M. I.; Zubieta, J. *Angew. Chem., Int. Ed.* **1994**, *33*, 760. (d) Khan, M. I.; Chang, Y.; Chen, Q.; Hope, H.; Parking, S.; Goshorn, D. P.; Zubieta, J. *Angew. Chem., Int. Ed.* **1992**, *31*, 1197. (e) Johnson, B. J. S.; Schroden, R. C.; Zhu, C. C.; Young, V. G.; Stein, A. *Inorg. Chem.* **2002**, *41*, 2213.

(5) (a) Kwak, W.; Rajkovic, L. M.; Stalick, J. K.; Pope, M. T.; Quicksall, C. O. *Inorg. Chem.* **1976**, *15*, 2778. (b) Chang, Y. D.; Zubieta, J. *Inorg. Chim. Acta* **1996**, *245*, 177. (c) Johnson, B. J. S.; Schroden, R. C.; Zhu, C. C.; Stein, A. *Inorg. Chem.* **2001**, *40*, 5972. (d) Liu, B. Y.; Ku, Y. T.; Wang, X. *Inorg. Chim. Acta* **1989**, *161*, 233. (e) Breen, J. M.; Schmitt, W. *Angew. Chem., Int. Ed.* **2008**, *47*, 6904.

(6) (a) DeBurgomaster, P.; Liu, H. X.; O'Connor, C. J.; Zubieta, J. *Inorg. Chim. Acta* **2010**, *363*, 3254. (b) Li, L.; Liu, B.; Xue, G.; Hu, H.; Fu, F.; Wang, J. *Cryst. Growth Des.* **2009**, *9*, 5206. (c) Darling, K.; Burkholder, E. M.; Pellizzeri, S.; Nanao, M.; Zubieta, J. *Inorg. Chem. Commun.* **2011**, *14*, 1745. (d) Onat, C. I.; Zhang, L.; Clerac, R.; Jean-Denis, J. B.; Feeney, M.; McCabe, T.; Schmitt, W. *Inorg. Chem.* **2011**, *50*, 604. (e) Soghomonian, V.; Slebodnick, C.; Spencer, E. C. *Dalton Trans.* **2010**, *39*, 8652.

(7) Izarova, N. V.; Dickman, M. H.; Biboum, R. N.; Keita, B.; Nadjo, L.; Ramachandran, V.; Dalal, N. S.; Kortz, U. *Inorg. Chem.* **2009**, *48*, 7504.

(8) (a) Xie, Y. P.; Yang, J.; Ma, J. F.; Zhang, L. P.; Song, S. Y.; Su, Z. M. *Chem.—Eur. J.* **2008**, *14*, 4093. (b) Xie, Y. P.; Ma, J. F.; Yang, J.; Su, Z. M. *Dalton Trans.* **2010**, *39*, 1568.

(9) Yi, F. Y.; Song, J. L.; Zhao, N.; Mao, J. G. *J. Solid State Chem.* **2008**, *181*, 1393.

(10) (a) Yi, F. Y.; Zhao, N.; Wu, W.; Mao, J. G. *Inorg. Chem.* **2009**, *48*, 628. (b) Yi, F. Y.; Xu, H. B.; Zhou, T. H.; Mao, J. G. *CrystEngComm* **2011**, *13*, 1480. (c) Yi, F. Y.; Lin, Q. P.; Zhou, T. H.; Mao, J. G. *J. Mol. Struct.* **2010**, *984*, 416. (d) Yi, F. Y.; Zhou, T. H.; Mao, J. G. *J. Mol. Struct.* **2011**, *987*, 51.

(11) Zhou, T. H.; Zhang, J.; Zhang, H. X.; Feng, R.; Mao, J. G. *Chem. Commun.* **2011**, *47*, 8862.

(12) Qian, X. Y.; Zhang, J. H.; Zhou, T. H.; Mao, J. G. *Dalton Trans.* **2012**, *41*, 1229.

(13) (a) Álvarez-Corral, M.; Muñoz-Dorado, M.; Rodríguez-García, I. *Chem. Rev.* **2008**, *108*, 3174. (b) Naodovic, M.; Yamamoto, H. *Chem. Rev.* **2008**, *108*, 3132.

(14) (a) Ford, P. C.; Vogler, A. *Acc. Chem. Res.* **1993**, *26*, 220. (b) Yam, V. W. W.; Lo, K. K. W. *Chem. Soc. Rev.* **1999**, *28*, 323.

(15) (a) *CrystalClear*, version 1.3.5; Rigaku Corp.: Woodlands, TX., 1999. (b) Sheldrick, G. M. *SHELXTL, Crystallographic Software Package, SHELXTL Version 5.1*; Bruker-AXS: Madison, WI, 1998. (c) Spek, A. L. *J. Appl. Crystallogr.* **2003**, *36*, 7.

(16) (a) Guo, L. R.; Bao, S. S.; Li, Y. Z.; Zheng, L. M. *Chem. Commun.* **2009**, 2893. (b) Guo, L. R.; Tong, J. W.; Liang, X.; Kohler, J.; Nuss, J.; Li, Y. Z.; Zheng, L. M. *Dalton Trans.* **2011**, *40*, 6392.

(17) (a) Guo, L. R.; Bao, S. S.; Li, Y. Z.; Zheng, L. M. *Chem. Commun.* **2009**, 2893. (b) Guo, L. R.; Tong, J. W.; Liang, X.; Kohler, J.; Nuss, J.; Li, Y. Z.; Zheng, L. M. *Dalton Trans.* **2011**, *40*, 6392.

(18) (a) Salta, J.; Chang, Y. D.; Zubieta, J. *J. Chem. Soc., Chem. Commun.* **1994**, 1039. (b) Mason, M. R.; Matthews, R. M.; Mashuta, M. S.; Richardson, J. F. *Inorg. Chem.* **1997**, *36*, 6476.

(19) (a) Sagatys, D. S.; Dahlgren, C.; Smith, G.; Bott, R. C.; White, J. M. *J. Chem. Soc., Dalton Trans.* **2000**, 3404. (b) Singleton, R.; Bye, J.; Dyson, J.; Baker, G.; Ranson, R. M.; Hix, G. B. *Dalton Trans.* **2010**, *39*, 6024. (c) Zavras, A.; Fry, J. A.; Beavers, C. M.; Talbo, G. H.; Richards, A. F. *CrystEngComm* **2011**, *13*, 3551.

(20) (a) Zheng, S. L.; Zhang, J. P.; Wong, W. T.; Chen, X. M. *J. Am. Chem. Soc.* **2003**, *125*, 6882. (b) Wang, C. M.; Wu, Y. Y.; Chang, Y. W.; Lii, K. H. *Chem. Mater.* **2008**, *20*, 2857.

(21) (a) Yang, J. H.; Zheng, S. L.; Yu, X. L.; Chen, X. M. *Cryst. Growth Des.* **2004**, *4*, 831. (b) Yan, C.; Chen, L.; Feng, R.; Jiang, F.; Hong, M. *CrystEngComm* **2009**, *11*, 2529. (c) Hu, M.; Zhang, Q.; Zhou, L. M.; Fang, S. M.; Liu, C. S. *Inorg. Chem. Commun.* **2010**, *13*, 1548.

(22) (a) Allendorf, M. D.; Bauer, C. A.; Bhakta, R. K.; Houk, R. J. T. *Chem. Soc. Rev.* **2009**, *38*, 1330. (b) Jin, J. C.; Wang, Y. Y.; Zhang, W. H.; Lermontov, A. S.; Lermontova, E.; Shi, Q. Z. *Dalton Trans.* **2009**, 10181.

(23) (a) Che, C. M.; Tse, M. C.; Chan, M. C. W.; Cheung, K. K.; Phillips, D. L.; Leung, K. H. *J. Am. Chem. Soc.* **2000**, *122*, 2464. (b) Omary, M. A.; Patterson, H. H. *J. Am. Chem. Soc.* **1998**, *120*, 7696. (c) Hou, L.; Li, D. *Inorg. Chem. Commun.* **2005**, *8*, 128. (d) Sun, D.; Liu, F. J.; Huang, R. B.; Zheng, L. S. *Inorg. Chem.* **2011**, *50*, 12393. (e) Catalano, V. J.; Munro, L. B.; Strasser, C. E.; Samin, A. F. *Inorg. Chem.* **2011**, *50*, 8465.

(24) Pramanik, S.; Zheng, C.; Zhang, X.; Emge, T. J.; Li, J. *J. Am. Chem. Soc.* **2011**, *133*, 4153.

(25) (a) Kyle, K. R.; Ryu, C. K.; Ford, P. C.; DiBenedetto, J. A. *J. Am. Chem. Soc.* **1991**, *113*, 2954. (b) Zhu, Q.; Sheng, T.; Tan, C.; Hu, S.; Fu, R.; Wu, X. *Inorg. Chem.* **2011**, *50*, 7618. (c) Shan, X. C.; Jiang, F. L.; Yuan, D. Q.; Wu, M. Y.; Zhang, S. Q.; Hong, M. C. *Dalton Trans.* **2012**, *41*, 9411. (d) Matsumoto, K.; Shindo, T.; Mukasa, N.; Tsukuda, T.; Tsubomura, T. *Inorg. Chem.* **2010**, *49*, 805. (e) Kitagawa, H.; Ozawa, Y.; Toriumi, K. *Chem. Commun.* **2010**, *46*, 6302. (f) Braga, D.; Maini, L.; Mazzeo, P. P.; Ventura, B. *Chem.—Eur. J.* **2010**, *16*, 1553.